

# Efficient Electromagnetic Analysis of Spiral Inductor Patterned Ground Shields

James C. Rautio, James D. Merrill, and Michael J. Kobasa

Sonnet Software, North Syracuse, NY, 13212, USA

**Abstract** — Patterned ground shields are widely used to increase the  $Q$  of spiral inductors on silicon. As RFIC (radio frequency integrated circuit) technology pushes toward deeper submicron nodes, the geometries of ground shields can become exceedingly complicated. This poses a huge challenge for numerical EM (electromagnetic) simulators. This paper explores several ground shield geometries and illustrates a new anisotropic conducting sheet model for efficient EM analysis of even the most complicated ground shield geometries by substitution of a continuous, but anisotropic conducting sheet. The technique is validated by comparison of EM analysis results using this new model to EM analysis results of actual ground shield geometries. We also explore visualization of the current induced in the silicon substrate by the inductor and (if present) the ground shield.

**Index Terms** — Anisotropy, CMOS technology, moment methods, numerical simulation, patterned ground, radio frequency integrated circuits, RFIC, spiral inductors.

## I. INTRODUCTION

Spiral inductors on silicon or other semiconducting substrates represent a major design challenge for the RFIC (radio frequency integrated circuit) designer. Efficient amplifier matching circuits and high quality VCO (voltage controlled oscillator) tuned circuits require inductors with the highest quality factor,  $Q$ . Achieving high  $Q$  given a large nearby semiconducting substrate is a challenge.

Spiral inductor substrate  $Q$  reduction results from two possible sources, e.g., [1], [2]. One source is inductive coupling to the conducting substrate. The conducting substrate can be viewed as creating a lossy image of the inductor below the substrate surface. This lossy image mutually couples with the actual inductor above the substrate to both reduce total inductance and to increase loss. Inductive effects modify the series branch of the usual spiral inductor pi-network model.

The other source for  $Q$  reduction is capacitive coupling between the inductor and the substrate. This can be viewed as displacement current (i.e., time-rate-of-change of the electric field) flowing through the insulator under the inductor. When the electric field reaches the substrate, it induces current in the substrate (by Ohm's law). This substrate induced current adds loss to the shunt branch of the spiral inductor Pi-network model. A patterned ground shield influences this shunt branch [3].

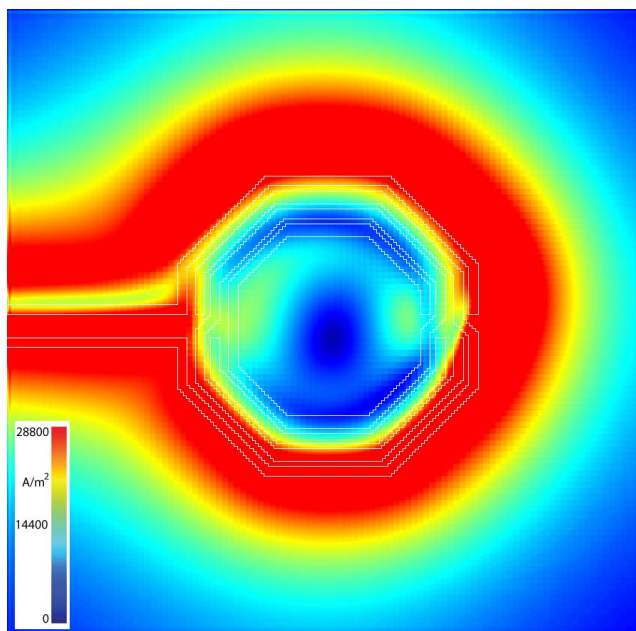


Fig. 1. Magnitude of the surface current distribution tangential to the top side of a silicon substrate under a spiral inductor shows unexpected results. For example, for this specific inductor, much of the current is outside the inductor area. As described later in this paper, the direction of the current is entirely unexpected.

Visualization of the currents induced in the surface of the substrate, for example, Fig. 1, can definitively and quantitatively determine which effect is dominant. Such visualization is detailed below. For the inductor considered here, capacitive effects are found to be dominant for substrate conductivities less than 80 S/m (1.25 Ohm-cm) with inductive effects dominant at higher conductivities.

With RFIC designs being pushed to deeper nodes, ground shield designs can and are becoming more complicated. In fact, their design can become so complicated that their inclusion can render an inductor design difficult or impossible to EM analyze. With this in mind, we developed a new anisotropic metal model for analysis of patterned ground shields of arbitrarily fine geometry. Below we illustrate and validate this approach. Then we explore visualization of the current induced in the surface of the semiconducting substrate with and

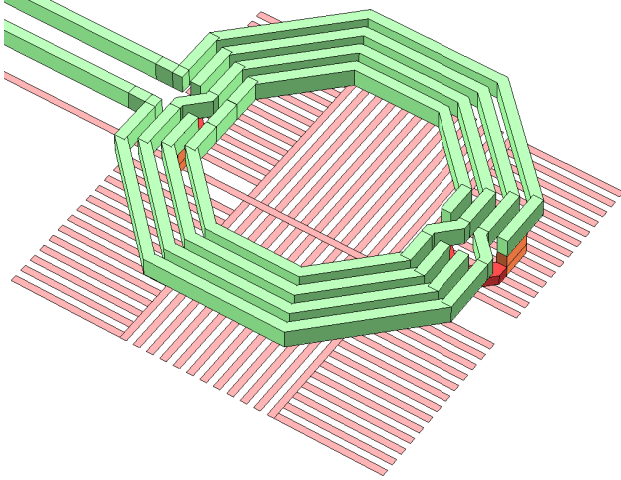


Fig. 2. Layout of the baseline inductor with a 2  $\mu\text{m}$  finger width and gap width patterned ground shield, to scale.

without a patterned ground plane, publishing such results, we believe, for the first time.

## II. INDUCTOR LOSS MECHANISMS

Inductor loss results from current flowing through the resistance of the inductor metal and from induced current flowing in the nearby lossy silicon substrate. To reduce the substrate loss, we can insert a ground plane between the silicon and the inductor to keep the inductor fields from entering the silicon.

A full ground plane is not effective because it results in an image of the inductor an equal distance below the ground plane. The inductor then inductively couples with its image, thus reducing the inductance and simultaneously increasing the metal loss. Thus, patterned ground shields are typically used.

The currents inductively induced in a full ground plane flow parallel to the currents flowing in the inductor. To eliminate this inductively induced current, slits are added in the ground plane perpendicular to the direction of current flow, or, in other words, perpendicular to the direction of the inductor's spiral turns. This allows the magnetic field circling the inductor turns to penetrate all the way to, and into, the substrate surface. Currents magnetically induced in the substrate cause image currents to flow, reducing the inductor's  $Q$  and inductance. The only remedies for this problem are to increase the substrate resistivity, or to move the substrate farther from the inductor.

The current induced in the substrate by the electric field, which is directed radially out from the inductor turns, obey the 3-D equivalent of Ohm's law, the constitutive relationship

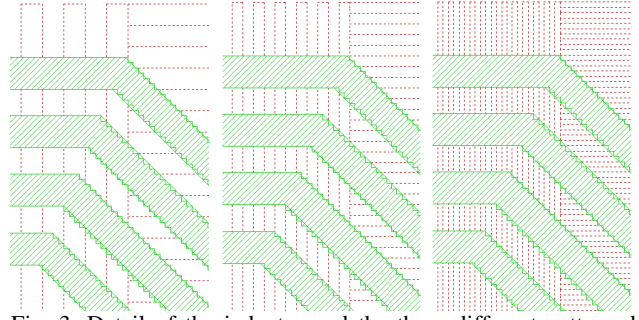


Fig. 3. Detail of the inductor and the three different patterned ground shields (dashed lines). From left to right both the finger width and gap width are 2, 1, and 0.5  $\mu\text{m}$ .

$$\mathbf{J} = \sigma \mathbf{E}, \quad (1)$$

where  $\mathbf{E}$  is the electric field (V/m) in the substrate,  $\sigma$  is the bulk conductivity (S/m), and  $\mathbf{J}$  is the resulting current density (A/m). Both  $\mathbf{J}$  and  $\mathbf{E}$  are three dimensional vectors. The patterned ground shield intercepts the portion of the inductor's electric field that is tangential to the surface of the substrate. The portion of the electric field that is perpendicular to the substrate is minimally affected by a patterned ground shield. The inductor's magnetic field, which does not encircle the patterned ground shield fingers, is likewise minimally affected.

The electric field tangential to surface of the substrate is the only source of inductor substrate loss that we can reduce by means of a patterned ground shield.

## III. THE BASELINE INDUCTOR

Fig. 2 shows the baseline inductor with a patterned ground shield with 2  $\mu\text{m}$  wide fingers and 2  $\mu\text{m}$  wide gaps. The inductor is 11  $\mu\text{m}$  above the ground shield with various dielectrics having an average  $\epsilon_{rel}$  of 4.2 in between. The ground shield is a fraction of a micron above the silicon substrate. The silicon bulk conductivity is 8.0 S/m (12.5 Ohm-cm). Several layers of passivation lie above the inductor metal. The lines are 3  $\mu\text{m}$  wide with gaps of 2.5  $\mu\text{m}$  using metal 2.8  $\mu\text{m}$  thick, conductivity  $3.4 \times 10^7$  S/m (2.9  $\mu\text{Ohm-cm}$ ), EM modeled with two sheets of current.

Fig. 3 shows a detail of the three patterned ground finger densities, 2.0, 1.0, and 0.5  $\mu\text{m}$ , with finger width equal to the gap. The patterned ground uses metal with conductivity  $2.3 \times 10^7$  S/m (4.3  $\mu\text{Ohm-cm}$ ), 0.5  $\mu\text{m}$  thick, EM modeled with a single sheet of current.

All EM analyses use Sonnet<sup>®</sup> [4]. The meshing cell size (i.e., the smallest possible subsection) is 0.5  $\mu\text{m}$ . For accurate capacitance calculation it is important that the

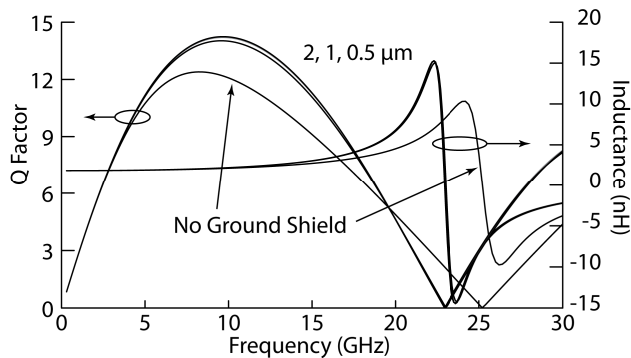


Fig. 4. Q and inductance for no ground shield and for the three ground shields of Fig. 3. The three ground shield inductance curves are essentially identical. The 0.5 and 1.0  $\mu\text{m}$  Q curves are almost identical (the 1.0  $\mu\text{m}$  curve is grey) and the 2  $\mu\text{m}$  curve is just below them.

maximum subsection size be no larger than the inductor line width. We conservatively set the maximum subsection size to half the inductor line width ( $Y_{\text{MAX}} = X_{\text{MAX}} = 3$  in Sonnet).

Fig. 4 shows the result for each of these ground shields and for no ground shield. Note that the ground shield lowers the resonant frequency from 25.2 GHz to 23.6 GHz. This is because it increases the capacitance to ground (see further comments below). The capacitance to ground is in parallel with the inductor and causes the first self-resonance to be a parallel LC resonance. The ground shield also increases the maximum Q from 12.4 to 14.2 and unexpectedly increases the frequency of maximum Q from 8.2 GHz to 9.2 GHz.

A key point to note is that using smaller finger widths (here, equal to the gap width) results in smaller increases in Q. In fact it appears to be approaching a limit with the 0.5 and 1.0  $\mu\text{m}$  Q curves almost exactly identical.

Before considering this limit, we investigated whether or not decreasing the finger-width-to-gap-width ratio effects Q. We evaluated a ground shield finger width of 2.0  $\mu\text{m}$  and a gap width of 0.5  $\mu\text{m}$ . The result was almost identical to the 2.0  $\mu\text{m}$  case of Fig. 3 and 4. It seems reasonable to conclude that as long as the gap is smaller than the finger width, the actual gap size has little influence, as noted in [3].

#### IV. THE ANISOTROPIC GROUND SHIELD MODEL

With the above, we can imagine that a small but finite finger width combined with a gap that goes to zero in the limit should yield essentially the same result as the 0.5  $\mu\text{m}$  finger width-gap case of Fig. 3 and 4.

This has two implications. First we could keep making the finger width and gap smaller and smaller and we should see essentially the same result as the 0.5  $\mu\text{m}$  case.

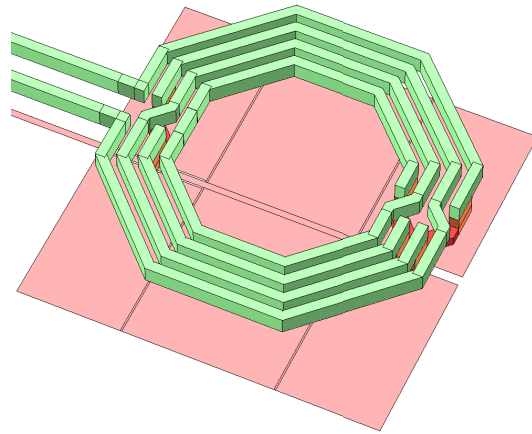


Fig. 5. The inductor layout with anisotropic metal substituted for the ground shield. This model gives results essentially identical to actually using a 1  $\mu\text{m}$  finger/gap width or smaller patterned ground shield.

This is what is happening as RFIC design encounters deeper nodes. Second, we can leave the finger width at 0.5  $\mu\text{m}$  and take the gap to zero width and we should see essentially the same result again.

We can easily take the finger gap to zero in EM analysis. This is done by using anisotropic metal. Anisotropic metal has one conductivity in one direction and a different conductivity in another direction. In this case, we use the regular metal conductivity in the direction of the fingers, and zero conductivity in the perpendicular direction. This technique was first described in [5].

Note that the inductor Q is insensitive to the value of the patterned ground conductivity. Reducing the patterned ground conductivity by half results in no discernible change in the result. The critical factor is that the patterned ground conductivity is a few orders of magnitude (in this case, six) higher than the silicon substrate. Inductor Q insensitivity to patterned ground resistivity also means that accurately modeling the edge singularity (i.e., the high current that flows on the edges of conductors) in the patterned ground is not needed. This allows use of a large subsection size in the patterned ground, whether it is the actual patterned ground, or an equivalent sheet.

Fig. 5 shows the spiral inductor with continuous anisotropic metal substituted for the finger arrays. As with the actual patterned grounds, we set the anisotropic metal maximum subsection size to half the inductor line width, assuring accurate calculation of the patterned-ground-to-inductor capacitance. In addition, the metal strips that connect the bases of all the fingers together are regular isotropic metal.

The results for this anisotropic metal model are visually identical (and are thus not presented) to the 0.5  $\mu\text{m}$  results

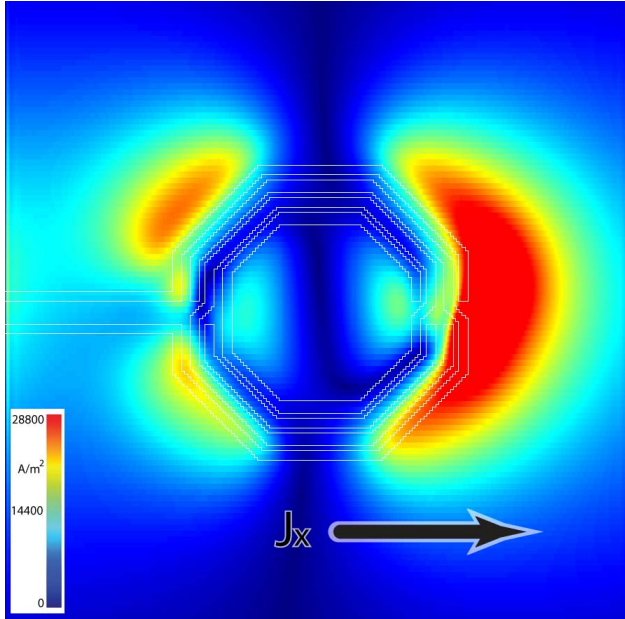


Fig. 6. With no ground shield, the  $x$ -directed (horizontal) substrate induced current flows only in the vicinity of the  $y$ -directed (vertical) inductor turns. It does not flow parallel to the inductor turns.

in Fig. 4, confirming the validity of the anisotropic metal patterned ground model.

Essentially, the anisotropic metal model can be used for any ground shield with any finger width and gap width as long as they are both small. In this case, small is anything less than  $1\ \mu\text{m}$  or so.

## V. SHUNT TO GROUND CAPACITANCE

The typical lumped model of an inductor includes a series branch that models the inductance, including resistance and capacitance. Then there are two shunt branches including capacitance and resistance. Both shunt branches connect to “Ground”. For the inductor plus ground shield of Fig. 2, Ground is the small strip below the two port lines. Since the port connecting line length (and ground strip) is removed by de-embedding, Ground is exactly and exclusively located on the ground strip where it passes into the inductor. Both ports have exactly the same Ground reference and the shunt to Ground capacitances from the inductor all go to that single and unique Ground.

Note that this is true in most lumped equivalent inductor models, both ports have exactly the same Ground reference and both shunt branches connect to this Ground. The impedance between the ground terminals is zero in the model and in the inductor.

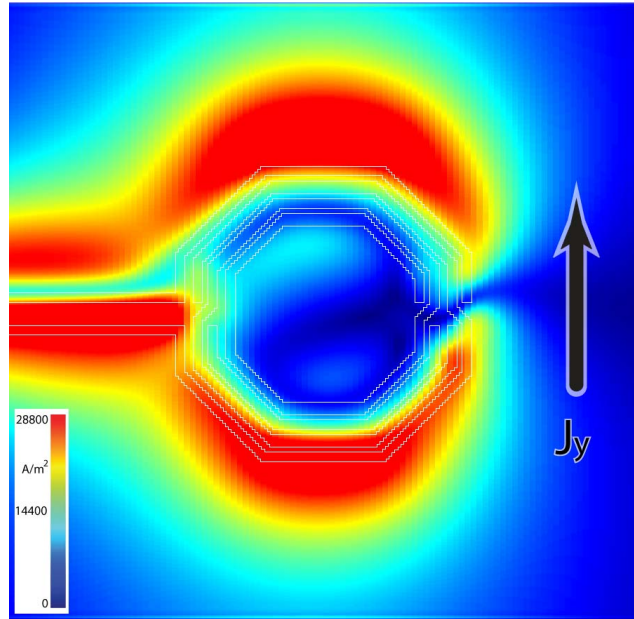


Fig. 7. With no ground shield, the  $y$ -directed (vertical) substrate induced current flows only in the vicinity of the  $x$ -directed (horizontal) inductor turns. It does not flow parallel to the inductor turns.

Problems arise when the actual inductor ports use different ground references. It is then possible for the inductor to insert current from one port into the ground terminal of another port. If we incorrectly assume both ports use exactly the same Ground reference, then negative valued lumped elements might be required in the equivalent lumped model. In this case, one should designate a single ground terminal as Ground, and all other ground terminals then become additional ports.

In addition, as mentioned in [3] and elsewhere, there should never be any kind of loop in the patterned ground shield. Not well known is that multiple connections between the ground shield and the rest of the embedding circuit can easily realize this undesired situation. A well designed inductor has one and only one Ground.

## VI. SUBSTRATE CURRENT VISUALIZATION

All current distribution plots in this paper show current density tangential ( $x, y$ ) to the surface of the substrate. Current flowing into or out of ( $z$ ) the substrate is not shown. In all cases, the inductors are excited by a  $1\ \text{V}$  source on port 1 with port 2 terminated in  $50\ \text{Ohms}$ .

Fig. 1 shows the total tangential surface current flowing in the substrate. A thin white outline shows the location of the inductor. Notice that most of the surface current is outside of the inductor. This indicates a large ground shield might provide improvement. In fact, when the

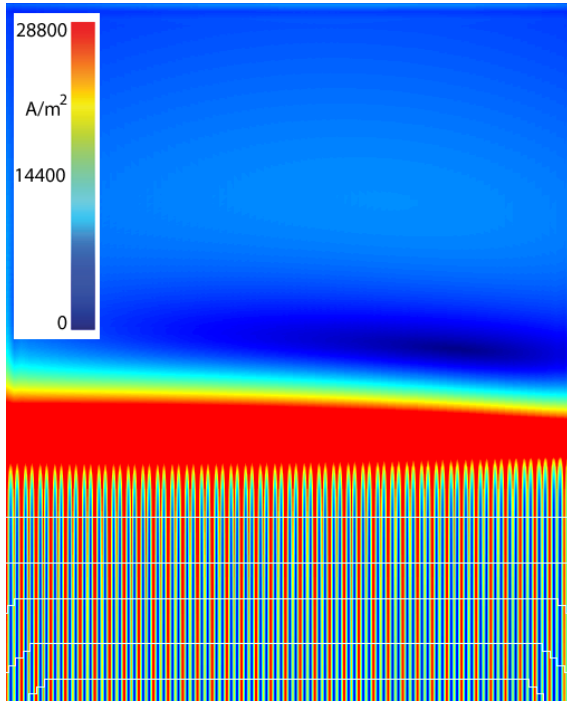


Fig. 8. Current capacitively induced in the surface of the substrate concentrates under the edges of the  $0.5\ \mu\text{m}$  wide fingers of a patterned ground shield. The narrow vertical bands of current are  $x$ -directed (horizontal) and the wide horizontal band in the middle is just outside the edge of the ground shield and is  $y$ -directed (vertical).

ground shield is extended an additional  $35\ \mu\text{m}$ , the maximum  $Q$  increases to 14.4.

Fig. 6 and 7 show the  $x$  and  $y$  components of the current induced by the inductor in the substrate surface. Note that there is no magnetically induced (i.e., parallel to the inductor turns) current. It is all capacitively induced current, flowing perpendicular to the inductor turns, driven by the electric field from the inductor. As noted in [1], high resistivity substrates tend not to have inductively induced currents. This can be quantitatively determined by viewing the direction of substrate surface current flow. We found that a substrate with  $80\ \text{S/m}$  ( $1.25\ \text{Ohm-cm}$ ) demonstrates a combination of inductive and capacitive currents, while  $800\ \text{S/m}$  ( $0.125\ \text{Ohm-cm}$ ) has predominantly inductively induced substrate currents. When the substrate currents are inductively induced, a patterned ground has almost no effect on  $Q$ .

Fig. 8 and 9 show the substrate surface current under a patterned ground shield ( $8\ \text{S/m}$  substrate conductivity). The strips of current are not under the ground shield fingers. Rather they are under the edges of the fingers and, driven by electric field from the fingers, they all flow perpendicularly to the fingers. Placing a secondary ground

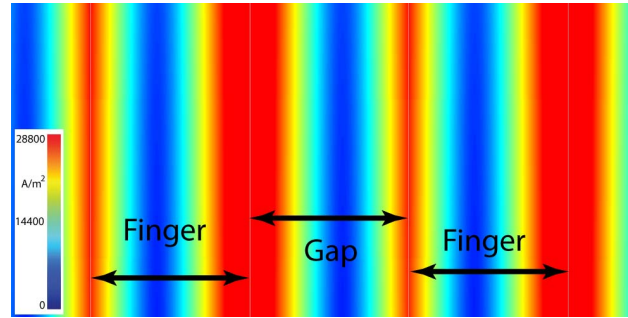


Fig. 9. Detail of the current in the substrate surface underneath the  $0.5\ \mu\text{m}$  patterned ground shield. Substrate current concentrates under the edges of the fingers. Here, each vertical band of current is  $x$ -directed (horizontal) and flows in the opposite direction of its immediately adjacent bands. The ground shield fingers are  $y$ -directed (vertical).

shield at the locations of these high current spots has little effect.

The wide horizontal band of current in the middle of Fig. 8 is just past the edge of the patterned ground. It is induced directly by the inductor and flows in the  $y$ -direction (vertical). All of these current directions are orthogonal to the direction we would expect from intuition. This is because they are induced by the electric field, not by the magnetic field.

## VII. CONCLUSION

We introduce and demonstrate the validity of the anisotropic metal model of patterned ground screens. We investigate the induced current in the surface of the substrate and find that for the considered inductor, all substrate current is capacitively induced and flows in the substrate in a direction perpendicular to the inducing current. We believe this is the first time that induced silicon substrate current visualization has been published.

## REFERENCES

- [1] W. B. Kuhn, et al., "Spiral inductor performance in deep-submicron bulk-CMOS with copper interconnects," in *IEEE MTT-S Int. Microwave Symp. Dig.*, 2002, pp. 301–304.
- [2] J. N. Burghartz and Rejaei, "On the Design of RF Spiral Inductors on Silicon," *IEEE Trans. Electron Devices*, vol. 50, No. 3, pp. 718–729, Mar. 2003.
- [3] C. P. Yue, and S. S. Wong, "On-chip spiral inductors with patterned ground shields for Si-based RF IC's," *IEEE J. Solid-State Circuits*, vol. 33, No. 5, pp. 743–752, May. 1998.
- [4] *Sonnet User's Manual, Version 14*, Sonnet Software, North Syracuse, NY, June 2011.
- [5] V. Mühlhaus, "Inductors with patterned ground shield in Sonnet," on line at [http://muehlhaus.com/wp-content/uploads/2011/06/Patterned\\_Ground\\_Inductor\\_Sonnet.pdf](http://muehlhaus.com/wp-content/uploads/2011/06/Patterned_Ground_Inductor_Sonnet.pdf).